Biochimica et Biophysica Acta, 596 (1980) 393—403

BBA 78646

MEASUREMENT OF NET PROTON-HYDROXYL PERMEABILITY OF LARGE UNILAMELLAR LIPOSOMES WITH THE FLUORESCENT pH PROBE, 9-AMINOACRIDINE

J. WYLIE NICHOLS [a], MARTYN W. HILL [b], ALEC D. BANGHAM [b] and DAVID W. DEAMER [a]

[a] *Department of Zoology, University of California, Davis, CA 95616 (U.S.A.) and* [b] *Agricultural Research Council, Institute of Animal Physiology, Babraham, Cambridge (U.K.)*

(Received May 4th, 1979)

Key words: Proton-hydroxyl permeability; Liposome; Fluorescent probe; 9-Aminoacridine

Summary

The fluorescent probe 9-aminoacridine was used to measure the rate of decay of experimentally established pH gradients across liposome membranes. From the rate of decay, separate permeability coefficients for protons (P_H) and hydroxyls (P_{OH}) were calculated and summed to yield the net proton-hydroxyl permeability (P_{net}). The net permeability of protons and hydroxyls was found to be approximately 10^{-4} cm/s, six orders of magnitude greater than that measured for sodium and pyrophosphate ions under similar conditions. This suggests that protons and/or hydroxyls cross lipid bilayers by a different mechanism than do other monovalent cations and anions. In addition, the measurements provide a standard for net proton-hydroxyl permeability in pure phospholipid bilayers for comparison with biological membranes.

Introduction

Liposomes provide a useful model system for studying numerous membrane related phenomena, including permeability of various biologically important ions. For instance, sodium, potassium, and chloride permeabilities have been measured using radioactive label methods [1—3]. However, the rapid equilibration of a tritium label between protons, hydroxyls and water makes it unsuitable for similar measurements of proton and hydroxyl permeabilities, and indirect methods are required.

Abbreviation: FCCP, carbonyl cyanide *p*-trifluoromethoxyphenylhydrazone.

We have used the fluorescent probe 9-aminoacridine to monitor pH gradients and their rate of decay across liposome membranes. From this decay rate, the net proton-hydroxyl flux can be calculated. The Goldman [4], Hodgkin and Katz [5] equation has been shown to predict accurately this measured flux and can be used to solve for the proton and hydroxyl permeability coefficients. These coefficients were summed to yield the net proton-hydroxyl permeability. Surprisingly, this net permeability was found to be six orders of magnitude greater than sodium permeability measured under similar conditions.

Although others have measured pH gradient decay [6—8] or combined proton-hydroxyl conductance [10—12] for membranous vesicles and bilayer membranes, to our knowledge this is the first report of net proton-hydroxyl permeability in liposomes.

Methods

Liposome preparation

Liposomes were prepared by an ether vaporization method described in detail elsewhere [13]. Diethyl ether solutions of phospholipid were injected into aqueous buffer solutions warmed to 60°C. The ether vaporized, and lipid dispersions with relatively high trapping-capacities (10—20 l/mol phospholipid) were formed. In typical experiments, 2 ml of ether solution of lipid (2 μmol/ml) were injected over a ten minute period into 4 ml of 30 mM pyrophosphate buffer (pH 5.5). Liposomes were prepared from 98 mol% phosphatidylcholine and 2 mol% phosphatidic acid (Avanti Biochemicals, Inc., Birmingham, AL). The resulting liposomes were filtered through a 0.45 μm Millipore filter to remove large lipid structures, followed by filtration through Sephadex G-50 (1 X 30 cm column) into 67 mM sodium sulfate (pH 5.5). The Sephadex beads were routinely removed from the column, washed in methanol and water, and repacked for each preparation.

The phospholipid and phosphate content of the liposomes was measured by the method of Raheja et al. [14] and Chen et al. [15], respectively. From the known phosphate concentration within the liposomes, the internal volume and the volume trapping efficiency of the liposomes were readily calculated. To produce a pH gradient of known magnitude, 0.2-ml aliquots of the liposome suspension were injected into 2.0 ml of isoosmotic buffers at pH ranges higher than the trapped buffer. The addition was made directly into the cuvet while in the fluorometer.

Measurement of pyrophosphate permeability

Liposomes were prepared containing pyrophosphate (PP_i) buffer (pH 5.5) inside and unbuffered Na_2SO_4 (pH 5.5) outside. The liposome solution was titrated to pH 8.5 with NaOH and placed on one side of a chamber separated by a dialysis membrane (exclusion size 12 000 mol. wt.). The solutions were stirred slowly and allowed to equilibrate for 4 h. The liposome solution, the dialysate, and a blank were then assayed for inorganic phosphate in order to determine pyrophosphate permeability. Phospholipid was extracted from the samples with chloroform/methanol (1 : 1). The remaining aqueous solution was dried and resuspended in 0.6 ml 0.5 N HCl, heated in a boiling water bath for

15 min to hydrolyze the pyrophoshate and assayed for inorganic phosphate [15].

Measurement of Na^+ permeability

When it was desired to compare sodium permeability to proton and hydroxyl permeability ^{22}Na was included in the internal buffer solution, and liposomes were prepared as usual, followed by gel filtration. The resulting suspension was placed in dialysis tubing and the rate of appearance of ^{22}Na was measured in the solution outside the dialysis membrane. This experiment was designed so that ^{22}Na and proton and hydroxyl permeability could be compared under similar conditions. We established concentration gradients of 1000 : 1 for protons, hydroxyls, and sodium. The proton and hydroxyl gradient was from $10^{-5.5}$ to $10^{-8.5}$ M and the sodium gradient was from 10^{-2} to 10^{-5} M. In this manner, the rate of sodium flux could be compared with that of protons and hydroxyls down similar gradients and under similar conditions. The ionic strength of the buffers was adjusted with potassium pyrophosphate (PP_i).

Measurement of ΔpH and proton-hydroxyl flux

ΔpH was measured using 9-aminoacridine, as previously described [16]. Twenty μl of 0.1 mM 9-aminoacridine in ethanol were placed in the cuvet of a recording Aminco Bowman spectrophotofluorometer containing 2.0 ml of aqueous buffer at varying pH values. The fluorescence (excitation 260 nm, emission 460 nm) was adjusted to 100% on the recorder, and the liposomes were added. Quenching of fluorescence indicated that the dye was taken up by the liposomes [16—19]. The fluorescence was recorded continuously for up to 40 min, and the relaxation of quenching was assumed to reflect the pH gradient decay by the combination of proton and hydroxyl flux. To be sure that 9-aminoacridine was not affecting the permeability of the liposomes, in other experiments the dye was added after efflux had occurred for varying intervals of time, and the quenching was compared with that obtained by continuous measurement. No significant differences were observed in the rate of ΔpH decay, and we concluded that 9-aminoacridine did not affect the proton and hydroxyl permeability of liposomes.

Net flux measurement

The relationship governing distribution of monoamines between membrane-enclosed volumes of different pH is [16]:

$$\Delta pH_{o-i} = pH_o - pH_i = \log \frac{A_i}{A_o} + \log \frac{V_o}{V_i} \qquad (1)$$

where ΔpH_{o-i} is the difference in pH inside (pH_i) and pH outside (pH_o). A_i and A_o are the total amount of amine inside and outside respectively, and V_i and V_o are the volumes inside and outside, respectively. Assuming the dye trapped inside the vesicles is totally quenched, A_i/A_o is given by $Q/(100 - Q)$, where Q is the percent quenching of the total fluorescence. This relationship was tested by varying the pH of the external buffer and calculating A_i/A_o from the measured values of Q. The plot of ΔpH versus $\log A_i/A_o$ is linear for ΔpH less

than 3 with a slope near the theoretical slope of 1.0. In order to account for any non-ideality in this system, for each set of liposomes the limits of linearity were tested, and a linear equation describing the relationship between ΔpH and log A_i/A_0 was determined and used to calculate the ΔpH for any given value of log A_i/A_0. The y-intercept of this line gives the theoretical value of log V_0/V_i. Thus, from the gradual increase in fluorescence, the value for log A_i/A_0 and ΔpH could be determined for a sequence of time points. Since the external solution is buffered sufficiently to maintain a constant pH, a change in ΔpH reflects a change in the internal pH alone, and the internal pH can be plotted against time. This graph was numerically differentiated to obtain dpH_i/dt vs. time. The buffer capacity of the internal buffer (B_i) can be determined from an acid or base titration experiment. The net change in internal proton concentration which is also equal to the net flux of protons and hydroxyls across the liposome membranes (J_{net}) can be calculated from the following relation:

$$J_{net} = \frac{dpH_i}{dt} \frac{B_i V_i}{A} \tag{2}$$

where V is the total internal volume, calculated by assaying the amount of pyrophosphate trapped inside the liposome, and A is the total surface area of the liposome, estimated by assaying the amount of phospholipid and assuming a packing area per molecule phospholipid of 55 A^2 [20]. In order to test our estimated values for internal volume (V_i) and surface area (A), we calculated the average diameter of a sphere having these properties from the relation $d = 6\ V_i/A$. The estimated diameter is 0.33 μm and is similar to the diameter (0.2 μm) calculated for ether-injected liposomes from negatively stained electron micrographs [21]. We conclude that the liposomes are primarily unilamellar and that our volume and area estimates are satisfactory.

Calculation of the net proton-hydroxyl permeability

The flux of protons and hydroxyls across a membrane can be expressed by the following equations derived by Goldman [4], Hodgkin and Katz [5].

$$-J_H = P_H \frac{VF}{RT} \frac{[H]_0 - [H]_i \exp(-VR/RT)}{1 - \exp(-VF/RT)} \tag{3}$$

$$-J_{OH} = P_{OH} \frac{VF}{RT} \frac{[OH]_i - [OH]_0 \exp(-VF/RT)}{1 - \exp(-VF/RT)} \tag{4}$$

J_H and J_{OH} are the net fluxes of protons and hydroxyls respectively; P_H and P_{OH}, the respective permeability coefficients; [H] and [OH], the proton and hydroxyl activities. The subscripts 'o' and 'i' refer to outside and inside, respectively. V is the electrical potential across the membrane.

J_{net} is determined from the change in the internal amount of protons per unit area per unit time, as described in the previous section, and reflects the combined net fluxes of protons and hydroxyls. Therefore:

$$J_{net} = P_H \frac{VF}{RT} \frac{[H]_0 - [H]_i \exp(-VF/RT)}{1 - \exp(-VF/RT)} + P_{OH} \frac{VF}{RT} \frac{[OH]_i - [OH]_0 \exp(-VF/RT)}{1 - \exp(-VF/RT)} \tag{5}$$

The electrical potential can be estimated by including all of the permeant

ions in the constant field equation [5].

$$V = \frac{RT}{F} \ln \frac{P_H[H]_i + P_{OH}[OH]_0 + P_{Na}[Na]_i + P_{PP_i}[PP_i]_0}{P_H[H]_0 + P_{OH}[OH]_i + P_{Na}[Na]_0 + P_{PP_i}[PP_i]_i} \quad (6)$$

Eqns. 5 and 6 are not readily solved analytically, therefore the following procedure was used to solve them. From each pH decay curve, the net flux at fifteen equally-spaced time points was calculated as described in the previous section. Since the external and internal pH are known for each time point, their respective activities can be calculated.

Initially, an arbitrary value for V was assumed, so that the independent variables for each time point could be substituted into Eqn. 5, resulting in a series of independent linear equations which could be solved by a least-squares analysis for the permeability coefficients P_H and P_{OH} [22]. These permeability coefficients, together with those previously measured for sodium and pyrophosphate, could then be substituted into Eqn. 6 to compute the electrical potential V for each time point. The values for V were used to write another series of equations from Eqn. 5 and solved for P_H and P_{OH} as before. This procedure was repeated until values for P_H and P_{OH} were found which satisfied both Eqns. 5 and 6. These separate coefficients were summed to yield the net proton-hydroxyl permeability (P_{net}). (Initial values for V were in the range of 30 mV and approached zero as ΔpH decayed.)

The validity of this analysis is dependent on the following assumptions. First, the use of the constant field equation depends on the basic assumptions used for its derivation [5]. In addition, we have assumed that the permeabilities of protons and hydroxyls are equal in both the inward and outward directions. This is a reasonable assumption considering that any surface charge asymmetry which might result from the different pH buffers in the inner and outer compartments would produce the same energy barrier to diffusion for ions passing in either direction, given a transmembrane voltage less than 80 mV [23]. We have also assumed that the permeabilities are constant over the pH range 5.5—6.5. The external pH remains constant while the internal pH changes from 5.5 to approx. 6.5. Over this range neither the egg phosphatidylcholine nor the phosphatidic acid have titratable charges [24]. It is therefore reasonable to assume that there are no significant changes in permeability resulting from the internal pH shift during the course of each experiment. Finally we have assumed that proton and hydroxyl flux through the lipid bilayer are separate and independent events.

Results

9-Aminoacridine and ΔpH measurements

Typical experimental data from a liposome system are shown in Fig. 1. Quenching under these conditions is entirely dependent on the existence of a pH gradient across the liposome membrane. Furthermore, when the amine has responded to an existing pH gradient, any condition which permits decay of the pH gradient also causes the fluorescence of the amine to return to its original level. These conditions include addition of 1 mM NH_4Cl, 0.1 mM

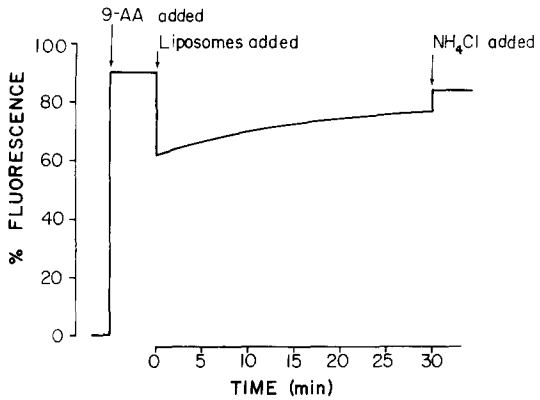

Fig. 1. Fluorescent measurement of pH gradient decay. Two ml of 30 mM $Na_4P_2O_7$ (pH 8.62) were placed in the cuvette of an Aminco Bowman Spectrofluorimeter. 20 μl 0.1 mM 9-aminoacridine was added and the fluorescence recorded, followed by addition of 0.2 ml of liposome solution (67 mM Na_2SO_4 (pH 5.82) outside; 30 mM $Na_2P_2O_7$ (pH 5.82) inside). Fluorescence was initially quenched, and gradually increased as the pH gradient decayed. 10 μl 100 mM NH_4Cl were added to release the pH gradient and allow measurement of total fluorescence in the absence of a gradient.

Triton X-100, nigericin, valinomycin + FCCP, or simply adding acid until the external pH approaches the internal pH. These diverse conditions provide strong qualitative evidence that 9-aminoacridine, under carefully chosen experimental conditions, responds to pH gradients by distributing into the acidic volume with consequent quenching of its fluorescence. The mechanism of fluorescence quenching is not yet understood.

The model described in Eqn. 1 predicts that the dependence of log A_i/A_0 should be linear with the pH of the external medium given that the internal pH and the amount of liposome solution added remain constant. As previously shown by others authors [16,18,19], this relationship is linear given a ΔpH of less than three pH units. The slope is close to the theoretical ideal of 1.0, and the y-intercept predicts a value for log V_0/V_i of 3.17, very close to that of 3.34 measured by the amount of trapped pyrophosphate buffer. Eqn. 1 also predicts a linear relationship between log V_0/V_i and log A_i/A_0. The relationship was tested and validated. We concluded that the fluorescence quenching of 9-aminoacridine could be used to measure ΔpH across liposome membranes.

Several investigators have questioned the validity of fluorescent probe analysis for measuring ΔpH. For instance, Massari [25] obtained anomalous fluorescence spectra when atebrin was permitted to interact with liposomes. On the basis of these results, Massari also criticized 9-aminoacridine as a probe of pH. However, Massari did not test 9-aminoacridine response to established pH gradients, as we have done here.

Kraayenhof [26] speculated that the pH dependence of acridine quenching does not result from amine distribution across membranes, but rather is due to titration of surface negative charges, so that the positively charged amine differentially interacts with the surface as pH is varied. A simple and direct test of Kraayenhof's proposed mechanism would be to determine whether positively

charged liposomes show quenching dependent on pH gradients. We have therefore tested liposomes containing 10 mol% cetyltrimethylammonium bromide, and found that 9-aminoacridine fluorescence is quenched, and that the pH dependence of the quenching is that expected from the standard relationships.

A more serious criticism of the 9-aminoacridine technique was raised by Fiolet et al. [18] who showed that the slope of the linear relationship between ΔpH and log A_i/A_0 is dependent in part on the concentration of negatively charged molecules in the liposome membranes. With this in mind, we chose to empirically determine the appropriate slope for each set of liposomes so that the calculated ΔpH and proton-hydroxyl flux rate would be independent of the lipid composition of the liposomes.

Permeability coefficients

Results from a typical experiment are shown in Figs. 2—4. The internal pH was calculated from the percent quenching of fluorescence [16] at regular time points after the addition of liposomes. The experimental conditions for these measurements were established such that all of the imposed pH gradients resulted in values for the percent quenching of fluorescence that fell within the limits of linearity established for Eqn. 1. These values were plotted (Fig. 2) and numerically differentiated (Fig. 3) so that the net flux (J_{net}) could be calculated from Eqn. 2 and plotted (Fig. 4). Since the external pH was buffered sufficiently to remain constant, the external and internal proton and hydroxyl concentrations at each time point could be derived from the internal pH plotted in Fig. 2. Fifteen linear equations of the form in Eqn. 5 were written and solved for P_H and P_{OH} by a least-squares analysis. The solid line in Fig. 4 represents the theoretically expected flux obtained by substituting the calculated values of P_H and P_{OH} into the theoretical flux equations. This theoretical curve correlates well with the experimental points.

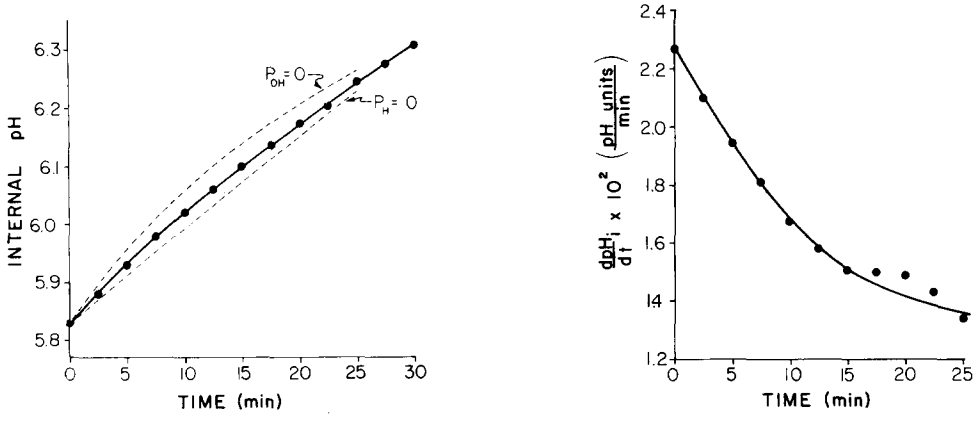

Fig. 2. Time course of internal pH of liposomes. Serial time points of A_i/A_0 from Fig. 1 were converted to ΔpH using Eqn. 1. Since the external pH was sufficiently buffered to remain constant, internal pH = ΔpH — external pH. The dotted lines represent the expected internal pH given the limiting cases such that there is no proton flux ($P_H = 0$) or no hydroxyl flux ($P_{OH} = 0$).

Fig. 3. Time course of the rate of change of internal pH. The curve in Fig. 3 was numerically differentiated and plotted to give dpH_i/dt vs. time [22].

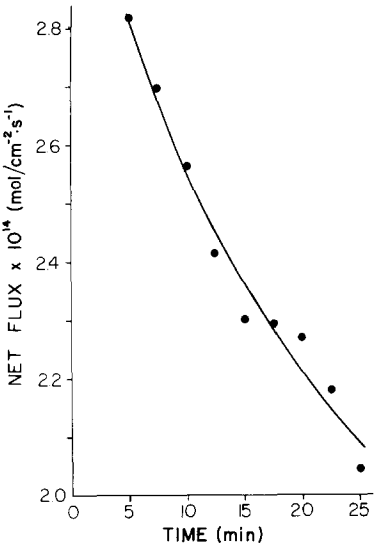

Fig. 4. Time course of net proton-hydroxyl flux. The values for dpH_i/dt in Fig. 3 were converted to net proton-hydroxyl flux by the following equation: $J_{net} = dpH_i/dt/$ [(buffer capacity) X (internal volume)/(surface area)]. The black dots (•) represent the calculated values for J_{net}. The solid line (———) was generated by substitution of the calculated values for P_H and P_{OH} into Eqn. 5.

In order to assess the sensitivity of this method for distinguishing between proton and hydroxyl permeability, we substituted the two limiting values for proton and hydroxyl permeability, $P_H = 0$ and $P_{OH} = 0$, into Eqn. 5 and calculated the expected flux vs. time for each case. These curves were numerically integrated to give the plot of pH_i vs. time for both limiting cases. These results are plotted in Fig. 2. As can be seen by comparing the two, small inaccuracies in computing the internal pH can result in large shifts in the calculated values of P_H and P_{OH}. For this reason, the separate permeability coefficients cannot be used to distinguish between proton and hydroxyl flux. However, their sum gives an accurate and reliable determination of the net proton-hydroxyl permeability.

P_{net} was found to be approx. 10^6 times greater than sodium permeability (P_{Na}) measured under the same conditions (Table I), and approximately 10 times less than the permeability of water ($0.8—18 \cdot 10^{-4}$ cm/s) measured from experiments based on the rate of swelling of multilamellar liposomes [27]. This value for P_{net} has been confirmed in our lab by a completely different technique using a glass pH electrode to monitor proton-hydroxyl flux (unpublished data).

However, our value for P_{Na} is considerably greater than previously reported values. Hauser et al. [3] measured $P_{Na} = 1.2 \cdot 10^{-14}$ cm/s in sonicated phosphatidylcholine vesicles, whereas Papahadjopoulos et al. [1] measured $P_{Na} = 1.1 \cdot 10^{-13}$ cm/s in sonicated vesicles containing 4% phosphatidic acid and 96% phosphatidylcholine. Our value for P_{Na} measured in ether-injected liposomes is 10^3 to 10^4 times greater. The reason for this large discrepancy is not clear, although it may result from the larger size of the ether-injected liposomes. The small size (0.05 μm average diameter) of the sonicated vesicles may impose

TABLE I

PERMEABILITY COEFFICIENTS FOR ETHER-INJECTED LIPOSOMES

Net proton-hydroxyl permeability was calculated as discussed in the text. The value for P_{net} is the mean ± S.D. Permeability for Na^+ and PP_i were calculated from the relation P = (fraction lost/s) × (internal volume)/(surface area).

Ions	Abbreviation	Permeability coefficient (cm/s)	Number of experiments
H^+ and OH^-	P_{net}	$1.4 \cdot 10^{-4} \pm 1.6 \cdot 10^{-4}$	8
Na^+	P_{Na}	$1.0 \cdot 10^{-10}$	1
Pyrophosphate (PP_i)	P_{PP_i}	$4.6 \cdot 10^{-11}$	1

physical constraints which result in lower ionic permeability.

Considering this difference in cation permeability between sonicated and ether injected liposomes, one would expect the proton-hydroxyl permeability to be significantly greater in the latter. We believe the larger vesicles to be a better model for most cellular membranes, whereas the sonicates more accurately reflect the properties of very small vesicular organelles.

The very low permeability of pyrophosphate (Table I) measured in the presence of a three-unit pH gradient eliminates the possibility that our flux measurements may have been influenced by protons or hydroxyls being transported bound to a pyrophosphate molecule. Pyrophosphate transport of protons cannot account for a significant amount of the measured flux.

In some experiments in order to rule out carbonic acid transport of protons, all of the buffer solutions were flushed with argon to remove carbon dioxide. P_{net} measured with and without argon did not differ significantly, and we concluded that carbonic acid was not responsible for transporting protons in this system.

We assumed that residual ether remaining in the liposomes preparation would affect their permeability properties to some degree. The amount of residual ether has been measured using radioactive ether as a tracer and found to be less than one millimolar [21]. An addition of 40 mM ether to the reaction mixture increased the net permeability 1.59 times over control. We therefore concluded that the amount of residual ether in the preparation had an insignificant effect on the measurement of permeability.

Other sources of contaminants which might have affected permeability were also tested. A portion of the stock phosphatidylcholine was purified by quantitative thin-layer chromatography and used to prepare liposomes. In addition, the commercial diethyl ether was distilled and peroxides were removed by shaking with a 5% aqueous ferrous sulfate solution [28]. In each case there was no significant difference in the flux rates as compared to the standard procedure. We concluded that the ether-injected liposome preparation accurately reflected the permeability properties of large unilamellar vesicles.

Discussion

Although others have measured proton and hydroxyl flux and conductance, this research reports the first attempt to quantify the net proton-hydroxyl

permeability of liposomes. Scarpa and DeGier [6] qualitatively measured the rate of pH decay in multilammellar liposomes. They measured the rate of change of pH in unbuffered solutions containing these vesicles in response to pH gradients and cation driven exchange and concluded that they were relatively impermeable to protons and hydroxyls. The very low proton-hydroxyl flux detected for these liposomes actually reflects a high permeability considering the exceptionally low concentrations of protons and hydroxyls in these solutions.

Mitchell and Moyle [9] used a similar technique to measure the effective proton conductance (combined proton and hydroxyl conductance) in mitochondria. They compared the mitochondrial effective proton conductance of 0.45 $\mu\Omega^{-1}/cm^2$ to that measured in artificial black lipid membranes of 0.1 $\mu\Omega^{-1}/cm^2$ measured by Thompson and collaborators [12] and concluded that mitochondria have the lowest natural membrane ion-conductance known. Ion conductance, though, is not a simple constant; it depends not only on the ion permeability of the membrane but also on the number and distribution of ions available on either side of the membrane. Since the number of protons and hydroxyls is very low compared to sodium, potassium and chloride ions, a low proton-hydroxyl conductance can still reflect a very large permeability coefficient.

Crandell et al. [8] used a pH pulse technique to determine the rate of pH equilibration across erythrocyte membranes. They assumed that hydroxyl ions could move through anion channels and therefore were solely responsible for the equilibration of imposed pH gradients. They concluded that the hydroxyl permeability varied with pH from $2 \cdot 10^{-4}$ at pH 9 to $4 \cdot 10^{-1}$ at pH 4. The assumption that protons do not flux across the erythrocyte membranes is questionable and leads to the calculation of an exceptionally large hydroxyl permeability coefficient at pH 4. If protons and hydroxyls are both assumed to flux, the net proton-hydroxyl permeability at pH 4 would be several orders of magnitude smaller than this calculated value for hydroxyl permeability alone.

Mechanism of proton-hydroxyl flux

The exceptionally high permeability coefficient calculated from proton-hydroxyl flux measurements suggests that proton equivalents must have a unique transport mechanism. One possible explanation which we are considering is that proton-hydroxyl flux is related to water content of the hydrophobic phase. It is clear that water exists within the lipid bilayer, since lipid membranes are relatively permeable to water, with permeability coefficients of the order of 10^{-3} cm/s [27,29,30]. Furthermore, water has a measurable solubility in bulk hydrocarbons in the millimolar range for *n*-alkanes [31]. Addition of a double bond increases water solubility even further, typically by 5—8 times when an alkane is compared with an alkene of the same chain length [31]. If it is assumed that some fraction of the water in the hydrophobic phase of lipid bilayers is associated, perhaps as hydrogen bonded strands entering from the membrane surface and extending into the interior, it is possible that protons and hydroxyl ions could in effect be transferred by rearrangement of the hydrogen bonds. This would provide a unique mechanism for proton-hydroxyl

transport not available to other monovalent cations and anions, and suggests further studies in which the degree of water association in hydrophobic phases will be determined.

Acknowledgements

The authors wish to thank Robert Macey for valuable discussion during the course of this work, and the Wellcome Trust for travel support. This study was supported by NSF grant BMS 75-01133.

References

1 Papahadjopoulos, D., Nir, S. and Ohki, S. (1972) Biochim. Biophys. Acta 266, 561—583
2 Johnson, S.M. and Bangham, A.D. (1969) Biochim. Biophys. Acta 193, 82—91
3 Hauser, H., Oldani, D. and Phillips, M.C. (1973) Biochemistry 12, 4507—4517
4 Goldman, D.E. (1943) J. Gen. Physiol. 27, 37—60
5 Hodgkin, A.L. and Katz, B. (1949) J. Physiol. (London) 108, 37—77
6 Scarpa, A. and DeGier, J. (1971) Biochim. Biophys. Acta 241, 789—797
7 Johnson, R.G. and Scarpa, A. (1976) J. Gen. Physiol. 68, 601—631
8 Crandell, E.D., Klocke, R.A. and Forster, R.E. (1971) J. Gen. Physiol. 57, 664—683
9 Mitchell, P. and Moyle, J. (1967) Biochem. J. 104, 588—600
10 Hopfer, V., Lehninger, A.L. and Thompson, T.E. (1968) Proc. Natl. Acad. Sci. U.S.A. 59, 484—490
11 Huang, C., Wheeldon, L. and Thompson, T.E. (1964) J. Mol. Biol. 8, 149—160
12 Maddy, A.H., Huang, C. and Thompson, T.E. (1966) Fed. Proc. 25, 933—936
13 Deamer, D.W. and Bangham, A.D. (1976) Biochim. Biophys. Acta 443, 629—634
14 Raheja, R.K., Kaur, C., Singh, A. and Bhatia, I.S. (1973) J. Lipid Res. 14, 695—697
15 Chen, P.S., Jr., Toribara, T.Y. and Warner, H. (1956) Anal. Chem. 28, 1756—1758
16 Deamer, D.W., Prince, R.C. and Crofts, A.R. (1972) Biochim. Biophys. Acta 274, 323—335
17 Rottenberg, H., Grunwald, T. and Avron, M. (1972) Eur. J. Biochem. 25, 54—63
18 Fiolet, J.W.T., Bakker, E.P. and Van Dam, K. (1974) Biochim. Biophys. Acta 368, 432—445
19 Casadio, R. and Melandri, B.A. (1977) J. Bioenerg. Biomembranes 9, 17—29
20 Luzzati, W. (1968) in Biological Membranes, Physical Fact and Function (Chapman, D., ed.), p. 71, Academic Press, New York, NY
21 Deamer, D.W. (1978) Ann. N.Y. Acad. Sci. 308, 250—258
22 Lanczos, C. (1961) Applied Analysis, 2nd edn., pp. 316—324. Prentice-Hall, Englewood Cliffs, NJ
23 Latorre, R. and Hall, J. (1978) in Membrane Transport Processes (Tosteson, D.C., Ovchinnikov, Y.A. and Latorre, R., eds.), Vol. 2, pp. 313—323, Raven Press, New York
24 Van Dijck, P.W.M., De Kruijff, B., Verkleij, A.J., Van Deenen, L.L.M. and DeGier, J. (1978) Biochim. Biophys. Acta 512, 84—96
25 Massari, S. (1975) Biochim. Biophys. Acta 375, 22—34
26 Kraayenhof, R. and Arents, J.C. (1977) in Electrical Phenomena at the Biological Membrane Level (Roux, E., ed.), pp. 493—505, Elsevier, Amsterdam
27 Bangham, A.D., DeGier, J. and Greville, G.D. (1967) Chem. Phys. Lipids 1, 225—246
28 The Merck Index (1976) (Windholz, M., ed.) 9th edn., p. 500, Merck and Co., Inc., Rahway, NJ
29 Hanai, T. and Haydon, D.A. (1966) J. Theor. Biol. 11, 370—382
30 Cass, A. and Finkelstein, A. (1967) J. Gen. Physiol. 50, 1765—1784
31 Schatzberg, P. (1965) J. Polym. Sci. Part C 10, 87—92
32 Black, C., Joris, G.C. and Taylor, H.S. (1948) J. Chem. Phys. 16, 537—543